Acta Oceanol. Sin., 2018, Vol. 37, No. 2, P. 14–24
DOI: 10.1007/s13131-017-1075-2
http://www.hyxb.org.cn
E-mail: hyxbe@263.net

Geochemical characteristics of major and trace elements in the Okinawa Trough basaltic glass

GUO Kun[1, 2, 3], ZHAI Shikui[3]*, YU Zenghui[3], ZENG Zhigang[1], WANG Xiaoyuan[1], YIN Xuebo[1]

[1] Key Laboratory of Marine Geology and Environment, Institute of Oceanology, Chinese Academy of Sciences, Qingdao 266071, China

[2] Laboratory for Marine Geology, Qingdao National Laboratory for Marine Science and Technology, Qingdao 266071, China

[3] Key Laboratory of Submarine Geosciences and Prospection of Ministry of Education, Ocean University of China, Qingdao 266100, China

Received 5 January 2017; accepted 16 May 2017

Abstract

The Okinawa Trough (OT) is a back-arc basin at an initial spreading stage that is under the influence of subduction of the Philippine Sea Plate. In this study, we analyzed the geochemical compositions of basaltic glass in the OT and discussed the effects of different magmatic sources, evolution, and subducted components in basalts. Our results showed that the middle and southern regions of the OT exhibit characteristics consistent with an iron-rich tholeiite series. Trace element proportions conform to the typical spider diagram pattern characteristic of back-arc basin basalts, rich in large ion lithophile elements (LILEs) including Rb, Ba, Pb, U, and Th, while depleted in high field-strength elements (HFSEs) including Nb, Ta, Zr, Hf, and Ti. The distribution of rare earth elements (REEs) is also consistent with enrichment by right-leaning light rare earth elements (LREEs). The addition of enriched mantle type I (EMI) materials as well as mantle heterogeneity may have led to variable degrees of enrichment in different regions. The magma source of the middle trough has undergone crystallization towards pyroxene, while development of plagioclase was restricted partly, and the crystallization of spinel and olivine ceased altogether. At the same time, crystallization of the southern OT magma source was dominated by olivine and including the formation of plagioclase, pyroxene, and magnetite (or titanomagnetite). Finally, the results of this study showed that 90% Th, 95% Ba in the southern basalt, 50%–70% Th and 70%–90% Ba in the middle basalt originated from subducted component. Different subducted component influence may be due to different subduction zone structural feature.

Key words: Okinawa Trough, basaltic glass, geochemistry, magmatic evolution, subducted component

Citation: Guo Kun, Zhai Shikui, Yu Zenghui, Zeng Zhigang, Wang Xiaoyuan, Yin Xuebo. 2018. Geochemical characteristics of major and trace elements in the Okinawa Trough basaltic glass. Acta Oceanologica Sinica, 37(2): 14–24, doi: 10.1007/s13131-017-1075-2

1 Introduction

It is well-known that the expansion model in back-arc basins is similar to the sea-floor spreading model in mid-ocean ridges (Karig, 1971). Although the major element compositions in back-arc basin basalts (BABBs) are similar to those of mid-ocean ridge basalts (MORBs), trace element and isotope compositions are different (Pearce and Stern, 2006). This variation is the result of the participation of fluids or/and melts derived from the subducting slab in the formation of BABBs. Although MORB-like lavas affected either a little or not at all by a component of subduction have been found in several back-arc basins (e.g., the Lau, Manus, and Shikoku basin as well as the Scotia Trough) (Eissen et al., 1991; Leat et al., 2000; Fretzdorff et al., 2002; Ishizuka et al., 2009), a number of other types and chemical compositions of lavas are known that have been affected by a subducted component. Because incompatible elements and volatiles in BABBs are intermediate in contents between MORBs and corresponding arc lavas, it is easy to consider the contribution of the subducted slab as a magma source for the former (Sinton et al., 2003). A number of researchers analyzed the effects of subducted slabs on BABB magma (e.g., Hawkins and Melchior, 1985; Pearce et al., 1994; Tian et al., 2008; Yu et al., 2016). Results showed that these magmas share a number of consistent geochemical characteristics; for example, compared to MORBs, BABBs contain more H_2O, alkali metals, and large ion lithophile elements (LILEs), while at the same time they are slightly depleted in Ti, Nb and Y. These magmas also conform to a smoother rare earth element (REE) model, where the total volume of these elements is between 5

Foundation item: The National Basic Research Program of China under contract No. 2013CB429702; the open fund project supported by the Laboratory for Marine Geology, Qingdao National Laboratory for Marine Science and Technology under contract No. MGQNLM-KF201707; the National Natural Science Foundation of China under contract Nos 41476044, 41325021 and 41306053; the Special Fund for the Taishan Scholar Program of Shandong Province under contract No. ts201511061; the AoShan Talents Program supported by Qingdao National Laboratory for Marine Science and Technology under contract No. 2015ASTP-0S17; the Innovative Talent Promotion Program under contract No. 2012RA2191; the Science and Technology Development Program of Shandong Province under contract No. 2013GRC31502.

*Corresponding author, E-mail: zhai2000@ouc.edu.cn

and 20 times that of chondrite.

Another important difference between BABBs and MORBs is that their magmas have experienced different modes of evolution (Niu, 2013). One major reason for this is the influence of H_2O on the order of crystallization of plagioclase and clinopyroxene in the magmatic system (Gaetani et al., 1993; Gaetani and Grove, 1998). Thus, MORBs can be considered as anhydrous basalt melts, depleted in incompatible elements and volatiles such as H_2O, while island arc basalts (IABs), including BABBs, can be considered as hydrous basalt melts that are rich in volatiles. Crystallization of plagioclase in an anhydrous (i.e., containing less H_2O) magma occurs earlier than clinopyroxene, while the reverse crystallized sequences in hydrogenous magma. In addition, in hydrous magmas, magnetite (or titanomagnetite) also crystallizes at an earlier stage of evolution (Pearce et al., 2005).

The Okinawa Trough (OT) is a back-arc basin in an initial spreading stage. The magmatism, including magma source addition of subducted slab materials and mode of eruption of crustal materials, is different from that at mid-ocean ridge spreading centers and in mature-type back-arc basins, with a number of unique properties (Guo et al., 2016). As a result, research on the geochemical composition of basalts can reveal the particular characteristics of back-arc basin magmatism in initial spreading stages. Although much research has been done on the magmatism of the OT (Sibuet et al., 1987; Ishizuka et al., 1990; Zhai and Gan, 1995; Li et al., 1997a, b; Shinjo et al., 1999; Chen et al., 2002; Ma et al., 2004; Hoang and Uto, 2006; Yan and Shi, 2014; Guo et al., 2016), a number of questions remain open, including the composition of the magma source, magmatic evolution, and effect of a subducted component. We evaluated basalt glass in this study as it reflects the properties of magma. To do this, we applied laser ablation-inductively coupled plasma-mass spectrometry (LA-ICP-MS) to measure the major and trace element compositions of basalt glass. In addition, based on the results of this study, we investigated the geochemical characteristics of the basaltic glass and the source materials for magmas, as well as evolutionary processes of crystallization and the effects of slab subduction on magmatism.

2 Geological background

The OT lies on the eastern margin of the continental shelf in the East China Sea, extending from the Kyushu Island, Japan, in the north to the Taiwan Island, China, in the south (Fig. 1). The OT comprises a complete trench-arc-basin system encompassing the Ryukyu Trench and Ryukyu Arc. The east and west sides of the OT are high angle normal faults that lean towards the trough axis, where parallel graben tectonics in line with the trend of the trough are also developed. The axis of this graben axis presents an en echelon arrangement on-and-off in a north-northeast direction and passes through the entire OT (Kimura, 1985). Overall, the trough is bounded by the Tokara (~130°E) and Miyako fault tectonic zones (~127°E), and is subdivided into southern, middle, and northern segments. The crustal thickness of the OT varies from 18 km in the south to about 30 km in the north (Shinjo and Kato, 2000; Liu et al., 2016), while the construction, magmatic characteristics, and geological conditions of the three segments are different (Huang et al., 2006). Indeed, a series of unique tectonic characteristics (e.g., tensional fault development, intense volcanic activity, abnormally high heat-flow values, crustal thicknesses intermediate between continental and oceanic crust) indicate that the OT is a young back-arc basin still within an initial spreading stage.

Volcanics within the OT conform to a bimodal distribution

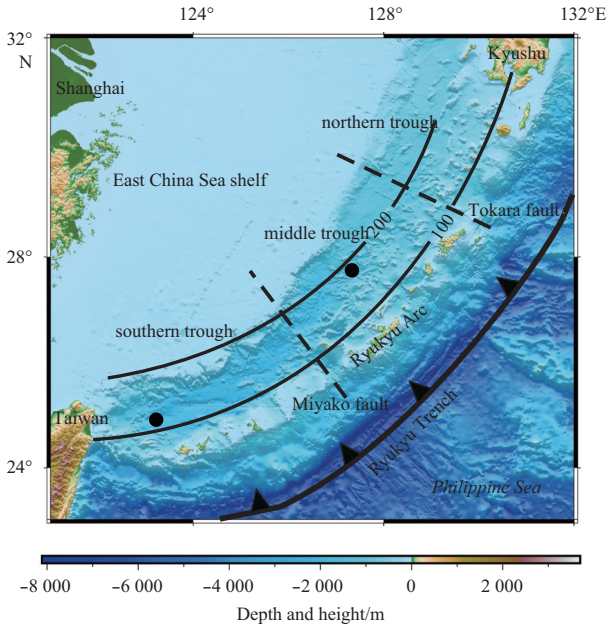

Fig. 1. Regional map of the OT inbasalt sampling locations. The black solid lines refer to the depth contours (100 and 200 km) of the Wadati-Benioff zone (Shinjo and Kato, 2000). The black solid circulars are basalt sample location. The black dash lines are Tokara and Miyako fault tectonic zones, respectively.

bounded by basic basalts and acidic rocks (Kimura et al., 1986; Honma et al., 1991). However, in comparison with the latter, there are limited basalt outcrop within the OT, mainly distributed in the middle and southern regions. A lot of research has been done on the petrology, mineralogy, element composition and isotopic geochemistry of the OT basalts (Kimura et al., 1986; Sibuet et al., 1987; Ishizuka et al., 1990; Zhai and Gan, 1995; Li et al., 1997a, b; Shinjo et al., 1999; Meng et al., 2000; Chen et al., 2002; Ma et al., 2004; Hoang and Uto, 2006; Yan and Shi, 2014). For example, Zhai and Gan (1995) investigated the mineralogy and chemical composition of basalts in the hydrothermal middle region of the OT (MOT) and concluded that these rocks comprise a tholeiite series. Because of the similarities with MORBs, they suggested that these rocks might be the result of sea-floor spreading. Based on the petrogeochemistry, Sr-Nd isotope compositions and mineralogical characteristics, Shinjo et al. (1999) and Chen et al. (2002) noted that the magma source of the OT is likely located within the superstrata of the upper mantle and variation in geochemical properties between the middle and southern basalts are most likely the result of tectonic differences between the two regions. The previous studies provide a foundation for further research on OT magmatism.

3 Materials and methods

The basalt samples used in this research were all fresh and come from sites in the middle and southern OT. Samples from MOT were obtained from a trawl carried out in 1992 by the Institute of Oceanography, Chinese Academy of Sciences, for the survey of hydrothermal activity, while samples from the southern trough (SOT) were acquired from a trawl carried out when the State Oceanic Administration conducted a geological and geophysical investigation of the OT in the summer of 1992. Sampling stations were located at 27°40′N, 127°20′E and 24°53.85′N, 123°12.25′E, respectively (Fig. 1). While Zhai and Gan (1995) and

Li et al. (1997b) investigated the chemical and mineralogical composition of these whole rock samples, we went further in this study to determine the in-situ compositions of major and trace element make-up of the host glass in two basalt samples using laser ablation inductively coupled plasma mass spectrometer (LA-ICP-MS). In addition, we reanalyzed the trace element compositions of whole rock basalt samples from the middle and southern OT.

Element analyses of silicate minerals using LA-ICP-MS were completed in the State Key Laboratory of Geological Processes and Mineral Resources, China University of Geosciences, Wuhan. During this process, we avoided crystalline minerals as much as possible; and used a Resonetics-M50 laser ablation system from RESOO Electronic Co. Ltd. A deep-ultraviolet 193 nm light beam generated by an ArF excimer laser generator was focused on mineral surfaces following light path homogenization. The laser beam spot diameter used was 33 μm, the ablation frequency was 10 Hz, and each cycle lasted 30 seconds. High purity helium (He) was used as the carrier gas and was pumped into the MS subsequent to mixing with argon (Ar) and a small amount of nitrogen (N). An iCAP Qc model ICP-MS from the Thermo Electron Corporation was used in this study while the National Institute for Standards and Technology (NIST) Standard Reference Material (SRM) 612 was used as the signal drift for correction. The NIST basalt glass international geological reference materials, BCR-2G, BHVO-2G, and BIR-1G, were utilized as external standards, while Si was used as the internal standard for measuring major and trace element contents. Replicate analyses on these standards showed that uncertainties are mostly less than ±4% of abundance, except for P (~9%). All test data were processed offline using the software ICPMSDataCal Version 9.9 (Liu et al., 2010a, b).

Trace elements compositions of whole rock samples were analyzed using ICP-MS in the Key Laboratory of Marine Geology and Environment, Institute of Oceanology, Chinese Academy of Sciences. About 40 mg of sample powders were placed in a PTFE bomb, and 1.5 mL of HF and 0.5 mL of HNO_3 were added. The sealed bombs were then placed in an electric oven and heated to 180°C for about 12 h. After cooling, the bombs were heated on a hot plate to evaporate and dry, and then 1 mL HNO_3 and 1 mL of ultrapure water were added. The bomb was again sealed and placed in an electric oven at 150°C for about 12 h for dissolving the residue. After cooling, the final dilute factor was about 1 000 for trace elements measurement by ICP-MS. The ICP-MS used for the analyses was an ELAN DRC II system from PerkinElmer Instruments Co. Ltd. Sampling (pore diameter: 1.1 mm) and skimmer cones (pore diameter: 0.9 mm) were both platinum, while the flow rates of atomized, auxiliary, and plasma gas in the Scott-crossed atomizing chamber were 0.82 L/min, 1.2 L/min, and 15 L/min, respectively. We used a lens pressure of 6 V, while the radio-frequency power of the ICP was 1 200 W and the pulse pressure was 1 250 V. Again, the international geological reference materials BCR-2, BHVO-2, AGV-2, and GSP-2 were used as standard samples and the internal standard was rhodium (Rh).

4 Geochemical characteristics

4.1 *Major element geochemistry*

The major element compositions of whole rock and basaltic glass samples from the OT are listed in Table 1. Results show that the composition of major elements in basaltic glass from the southern trough remains relatively uniform, similar to whole rock samples. However, basaltic glass samples from the middle trough exhibit slightly different major element compositions compared to the whole rock. For example, while the SiO_2 content of glass is higher than that of whole rock samples, the MgO content is lower. Based on the total-alkali-silica (TAS) diagram (Fig. 2), it is clear that the southern basalt, glass, and middle trough basalt all fall within the range of the basalt, while the middle basaltic glass falls within the range of a basaltic andesite, indicating the existence of crystallization differentiation. In K_2O-SiO_2 diagram (Fig. 3a), it is clear that the middle basalt and glass plot close to the boundary line between a medium-to-low-K series, while the southern basalt and glass fall within a medium-K series. Based on the AFM diagram (Fig. 3b), the middle and southern basalt and glass all plot near to the boundary between tholeiitic and calc-alkaline series, while at the same time exhibiting an evolutionary trend characteristic to an iron-rich tholeiitic series. These results indicate that the basalt magma in the OT can be classified as a tholeiitic series (Miyashiro, 1974).

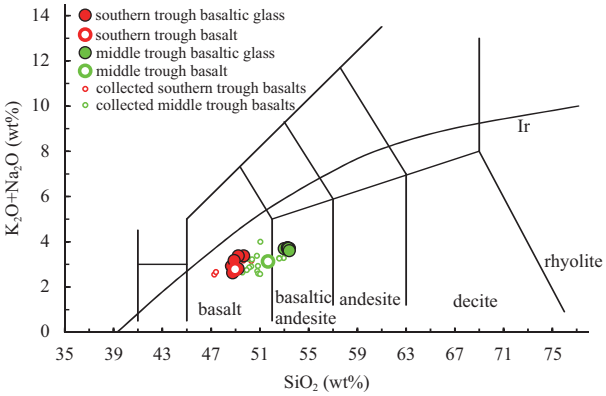

Fig. 2. TAS diagram for OT basalt and basaltic glass samples (adapted from Rickwood, 1989). Collected Okinawa Trough basalts data is from Li et al. (1997a, b), Shinjo et al. (1999), Ma et al. (2004), and Hoang and Uto (2006).

4.2 *Trace element geochemistry*

Trace element compositions of basalt and basaltic glass samples from the OT are shown in Table 1. In order to easily compare the distributions of trace elements in basaltic glass samples, average values were chosen for N-MORB standardization (Sun and McDonough, 1989), and a spider diagram was plotted (Fig. 4). The results of this characterization show that the middle and southern basalts as well as basaltic glass all exhibit trace element distribution patterns typical of BABBs, rich in LILEs, such as Rb, Ba, Pb, U, and Th, and depleted in HFSE, such as Nb, Ta, Zr, Hf, and Ti (Sinton et al., 2003). Of these, Nb, Ta, Zr, and Hf as well as heavy REEs (HREEs) are more depleted in samples of the southern basalt and basaltic glass than they are in samples of the middle basalt and basaltic glass. However, Rb, Ba, K, U, and Sr are all more abundant in the middle basalt and basaltic glass; in general, trace element contents in basaltic glass samples are higher than they are in the whole rock, likely the result of differences in magmatic evolution.

4.3 *Rare earth element geochemistry*

Measured REE compositions of whole rock and basaltic glass samples from the OT are shown in Table 1. These results show that the ΣREE of basaltic glass from MOT is 76.98×10^{-6} on average. All values and ratios of basaltic glass are on average higher than the southern basaltic glass (68.45×10^{-6}), while the ΣREE of

basalt (60.53×10^{-6}) is also higher than these southern samples (52.12×10^{-6}). Average values of chondrite-normalized basaltic glass as well as the basalt spider diagram for REEs are shown in Fig. 5; these results show that both whole rock and basaltic glass samples contain right-leaning light REEs (LREEs) enrichment characteristics. For example, La_N/Yb_N=2.71 and δEu=1.08 for the middle basalt, while for basaltic glass these are 2.11 and 0.91, respectively. In contrast, La_N/Yb_N and δEu values for the southern

Table 1. The major trace elements of basaltic glass and whole rock analyzed in this study

Middle trough	Basaltic glass									Whole rock
	B-1-1	B-1-2	B-1-3	B-1-4	B-1-5	B-1-6	B-1-7	B-1-8	B-1-9	
SiO_2	53.40	53.33	52.98	53.25	53.39	53.24	53.31	53.31	53.39	51.64
TiO_2	1.27	1.42	1.42	1.43	1.41	1.26	1.34	1.35	1.42	1.00
Al_2O_3	16.17	14.49	14.57	14.73	14.57	15.97	15.05	15.26	14.29	16.16
FeOt	9.71	10.95	10.98	10.92	10.79	9.93	10.51	10.52	11.10	9.21
MnO	0.20	0.23	0.23	0.23	0.22	0.20	0.21	0.21	0.23	0.18
MgO	4.65	5.32	5.36	5.12	5.24	4.79	5.26	4.95	5.49	7.21
CaO	10.17	9.77	9.95	9.77	9.89	10.15	9.89	9.90	9.65	9.80
Na_2O	3.24	3.12	3.15	3.16	3.12	3.23	3.12	3.18	3.07	2.73
K_2O	0.49	0.58	0.57	0.59	0.57	0.51	0.55	0.54	0.56	0.42
P_2O_5	0.27	0.30	0.30	0.31	0.31	0.28	0.29	0.29	0.30	0.19
Total	99.56	99.51	99.51	99.51	99.51	99.55	99.53	99.53	99.50	98.54
Li	6.09	7.77	7.67	7.51	7.69	6.80	7.16	7.16	7.37	5.20
Be	1.00	0.80	0.65	0.95	0.93	0.80	0.67	0.96	1.23	0.61
Sc	40.82	45.15	46.19	43.99	45.55	41.61	43.37	42.48	45.59	25.18
V	320.39	365.69	371.31	361.31	364.32	326.96	347.10	345.13	365.58	238.56
Cr	63.11	73.63	79.43	69.41	74.21	63.54	68.09	66.18	75.33	221.12
Co	26.71	31.00	31.19	30.08	30.31	27.50	30.18	29.72	31.28	38.62
Ni	14.43	15.81	16.08	14.67	15.74	13.85	17.33	14.52	17.37	116.90
Cu	65.35	81.40	76.76	78.70	80.32	71.75	76.86	74.55	79.15	84.62
Zn	84.23	99.76	98.17	101.12	99.80	88.66	93.05	95.73	97.57	117.78
Ga	18.67	18.14	18.01	18.14	18.21	18.98	18.07	18.27	17.97	16.89
Rb	9.20	11.30	10.90	11.46	11.06	9.79	10.79	10.55	11.13	7.50
Sr	239.29	212.67	212.39	216.65	215.14	238.82	220.94	226.57	210.27	239.91
Y	29.08	32.07	33.02	32.12	32.62	28.90	30.83	31.26	32.72	25.53
Zr	94.73	106.62	106.49	107.34	106.37	95.91	101.69	102.48	107.40	81.85
Nb	4.08	4.52	4.41	4.62	4.68	4.08	4.59	4.42	4.66	3.22
Mo	0.45	0.40	0.58	0.56	0.50	0.49	0.55	0.52	0.67	2.08
Sn	1.87	2.15	2.14	2.02	1.92	1.55	2.06	1.89	2.08	—
Cs	0.44	0.56	0.56	0.57	0.54	0.45	0.50	0.54	0.58	0.35
Ba	99.51	110.83	110.32	113.60	108.77	99.82	106.52	106.95	109.97	104.57
La	8.67	9.62	9.83	9.76	9.38	8.64	9.33	9.54	9.77	8.86
Ce	21.12	23.78	23.67	24.22	23.54	21.21	22.72	23.24	23.96	18.56
Pr	3.11	3.36	3.35	3.47	3.33	3.00	3.25	3.27	3.39	2.67
Nd	14.51	15.96	15.96	15.87	15.64	14.10	14.82	15.66	15.88	11.81
Sm	3.93	4.46	4.53	4.41	4.68	4.01	4.22	3.82	4.46	3.28
Eu	1.35	1.51	1.42	1.41	1.39	1.28	1.40	1.39	1.37	1.15
Gd	4.65	5.21	5.46	4.94	5.18	5.04	5.06	5.02	5.41	3.28
Tb	0.74	0.80	0.87	0.87	0.86	0.80	0.80	0.81	0.85	0.62
Dy	5.11	5.70	5.57	5.67	5.70	5.15	5.63	5.62	5.64	3.89
Ho	1.09	1.19	1.18	1.18	1.15	1.06	1.13	1.13	1.18	0.87
Er	3.27	3.52	3.60	3.60	3.47	3.06	3.33	3.46	3.54	2.44
Tm	0.43	0.50	0.49	0.51	0.51	0.44	0.48	0.49	0.51	0.38
Yb	2.81	3.27	3.38	3.17	3.39	2.90	3.03	3.31	3.46	2.34
Lu	0.45	0.53	0.51	0.51	0.52	0.46	0.49	0.53	0.51	0.37
Hf	2.36	2.67	2.65	2.62	2.75	2.33	2.60	2.67	2.69	1.93
Ta	0.22	0.26	0.30	0.27	0.26	0.21	0.26	0.25	0.30	0.17
W	0.15	0.15	0.13	0.14	0.17	0.11	0.14	0.15	0.17	0.27
Pb	5.80	3.15	3.14	3.30	3.19	2.75	3.02	3.29	3.13	7.00
Th	0.98	1.05	1.11	1.08	1.09	0.98	1.03	1.06	1.08	0.81
U	0.25	0.28	0.27	0.30	0.29	0.24	0.28	0.27	0.27	0.33

to be continued

Continued from Table 1

Southern trough	Basaltic glass						Whole rock
	B-2-1	B-2-2	B-2-3	B-2-4	B-2-5	B-2-6	
SiO_2	48.66	49.20	49.65	48.74	49.21	48.87	48.94
TiO_2	1.21	1.03	1.19	1.04	1.01	1.17	0.87
Al_2O_3	15.17	15.60	14.18	15.50	16.89	14.97	17.33
FeOt	10.84	9.56	11.33	9.18	9.69	11.09	9.62
MnO	0.23	0.20	0.25	0.20	0.19	0.23	0.19
MgO	6.96	6.71	6.86	7.26	6.32	6.59	6.80
CaO	13.23	14.18	12.31	14.72	12.56	13.10	12.27
Na_2O	2.30	2.33	2.54	2.20	2.66	2.55	2.19
K_2O	0.65	0.51	0.86	0.45	0.74	0.65	0.62
P_2O_5	0.26	0.23	0.30	0.25	0.27	0.26	0.26
Total	99.50	99.54	99.48	99.56	99.54	99.48	99.09
Li	4.11	2.57	3.98	3.31	3.89	4.37	3.43
Be	0.72	0.60	0.91	0.38	0.78	1.06	—
Sc	43.92	46.22	42.61	44.65	37.11	43.49	29.62
V	407.42	369.23	404.79	381.49	320.54	413.20	257.27
Cr	7.48	20.09	6.04	10.32	7.06	6.11	67.30
Co	37.45	35.45	40.28	36.01	35.03	39.26	41.65
Ni	19.39	22.79	20.61	25.62	22.83	19.06	64.74
Cu	121.70	99.61	126.90	87.41	145.91	121.32	101.03
Zn	67.20	58.47	69.91	53.07	47.44	61.94	82.36
Ga	16.76	17.00	16.65	17.06	17.49	16.94	15.69
Rb	11.23	8.46	13.36	7.75	12.40	12.16	8.83
Sr	306.70	348.55	307.45	344.06	352.05	356.92	363.87
Y	24.86	21.69	25.43	21.89	21.33	24.10	16.64
Zr	73.61	61.87	78.21	63.74	68.48	72.71	54.50
Nb	2.63	1.99	2.96	1.85	2.98	2.48	2.01
Mo	0.36	0.31	0.57	0.31	0.50	0.34	0.67
Sn	2.63	1.52	1.81	1.56	1.78	1.63	—
Cs	0.39	0.30	0.56	0.29	0.51	0.41	0.36
Ba	228.12	193.03	253.68	164.05	228.05	219.52	200.46
La	10.05	8.70	11.70	7.78	10.25	10.09	6.86
Ce	22.03	18.99	24.99	18.14	21.49	22.05	14.76
Pr	3.11	2.74	3.38	2.63	2.93	3.07	2.22
Nd	14.19	12.79	15.70	12.71	13.01	14.39	9.85
Sm	3.84	3.53	4.07	3.58	3.29	3.94	2.64
Eu	1.35	1.19	1.31	1.24	1.14	1.33	0.98
Gd	4.48	3.89	4.43	4.01	3.75	4.24	2.51
Tb	0.73	0.63	0.74	0.60	0.55	0.70	0.48
Dy	4.43	4.10	4.63	4.25	3.98	4.23	2.72
Ho	0.96	0.84	0.92	0.85	0.78	0.89	0.59
Er	2.79	2.49	2.75	2.44	2.29	2.65	1.60
Tm	0.42	0.33	0.41	0.37	0.34	0.37	0.26
Yb	2.57	2.30	2.59	2.20	2.21	2.57	1.58
Lu	0.43	0.37	0.39	0.36	0.33	0.38	0.25
Hf	2.02	1.73	2.00	1.68	1.71	1.76	1.29
Ta	0.17	0.15	0.20	0.13	0.16	0.17	0.11
W	0.14	0.11	0.23	0.09	0.19	0.13	0.19
Pb	2.75	2.14	3.64	1.73	4.13	2.10	4.15
Th	2.37	1.91	2.65	1.80	2.20	2.20	1.56
U	0.44	0.36	0.50	0.32	0.51	0.42	0.38

Note: Data of whole rocks in middle and southern trough is from Zhai and Gan (1995) and Li et al. (1997b), respectively. Major elements oxides in 10^{-2}. Trace elements in 10^{-6}. FeOt is total Fe, expressed as Fe^{2+}.

basalt are 3.12 and 1.17, respectively, while La_N/Yb_N and δEu for basaltic glass from SOT are 2.91 and 0.98, respectively. The slopes of REE distribution curves of the southern basalt and basaltic glass are steeper than the corresponding samples from MOT. Overall, as is the case for trace elements, the contents of REEs in basaltic glass samples are higher than these of the whole rock,

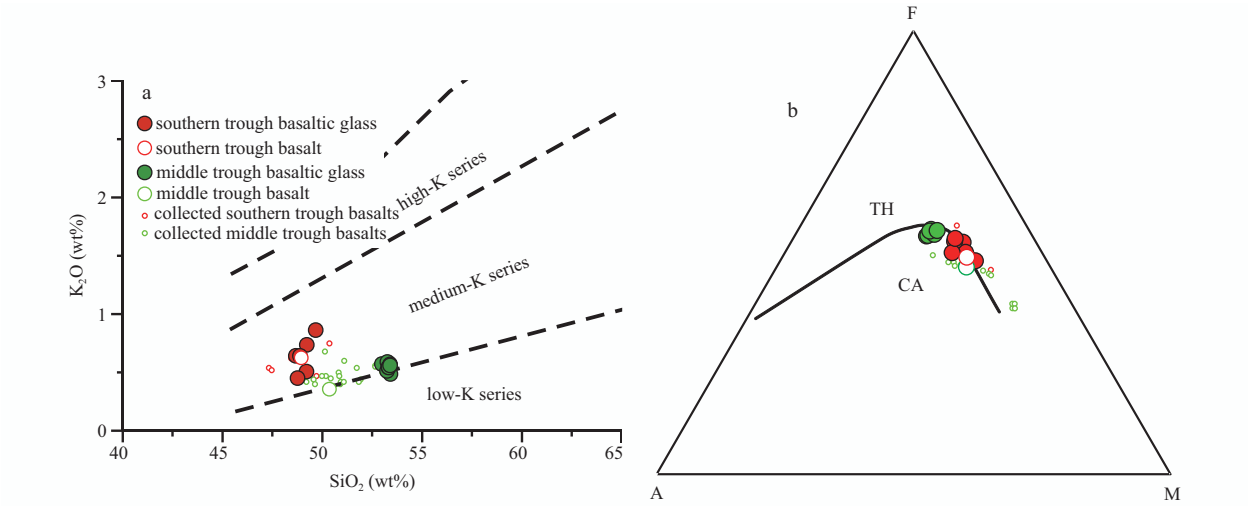

Fig. 3. K_2O-SiO_2 (a) and AFM diagrams (b) for OT basalt samples. TH indicates tholeiite basalt series, and CA calc-alkali basalt series. Two diagrams are adapted from Rickwood (1989) and Miyashiro (1974), respectively. Okinawa Trough basalts data is from Li et al. (1997a, b), Shinjo et al. (1999), Ma et al. (2004), and Hoang and Uto (2006).

again a likely consequence of magmatic evolution.

5 Discussion

5.1 *Magma source characteristics*

It is clear from the trace element spider diagram (Fig. 4) that basalt and basaltic glass samples from the MOT and SOT exhibit similar characteristics. At the same time, however, these samples differ in the proportions of the elements Nb, Ta, Zr, and Hf, as well as HREEs which can be used to characterize the original magma source. Results show that samples of basalts and basaltic glass from SOT are more depleted in these elements than samples from MOT, which indicates that the southern magma source is more depleted overall than that in the MOT. In addition, as HFSEs are hard to dissolve in water and exhibit stable chemical properties, they are often used as indicators of the compositional characteristics of "original" material (Leat et al., 2000). Thus, in this context, the ratio between Zr and Nb can be used to some extent to reflect mantle source characteristics. For example, this ratio is 22.17–24.16 (average: 23.20), in samples of basalt and basaltic glass from the MOT, 22.96–34.39 in basaltic glass from SOT (average: 28.68). These data indicate that the main magma source for these regions is N-MORB-type mantle (Zr/Nb=31.76), although a small amount of enrichment-type mantle may also be included (e.g., Zr/Nb of E-MORB is 8.80; Sun and McDonough, 1989). Thus, in the context of a middle mantle source, southern mantle source is more depleted.

Normalizing the ratio of HFSE using Yb means that the effects of partial melting and fractional crystallization on element content can be reduced or eliminated, and the geochemical characteristics of mantle source can be determined (Macdonald et al., 2000). The normalized Ta, Zr, and Hf using Yb are presented in Fig. 6; and results show that basalt from MOT as well as basaltic glass plot is farther away from the N-MORB end member and there are more enrichment than basalt in SOT as well as basaltic glass. This finding is consistent with the trace element spider diagram for these samples (Fig. 4) as well as with the ratio between Zr and Nb. Variable contributions of EMI-type mantle materials to the magma source of the middle OT may be the reason for the different degrees of enrichment in the middle and southern

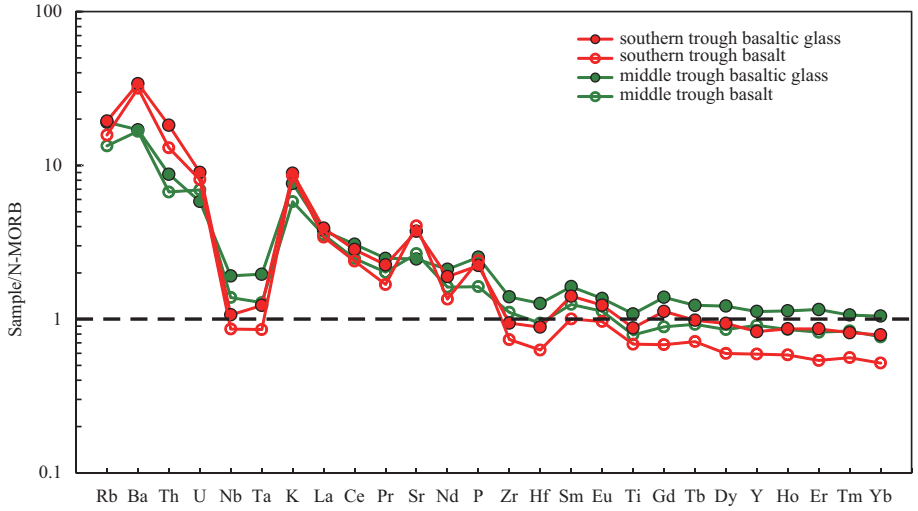

Fig. 4. N-MORB-normalized diagram of trace elements in basalt and basaltic glass samples from the OT (Sun and McDonough, 1989).

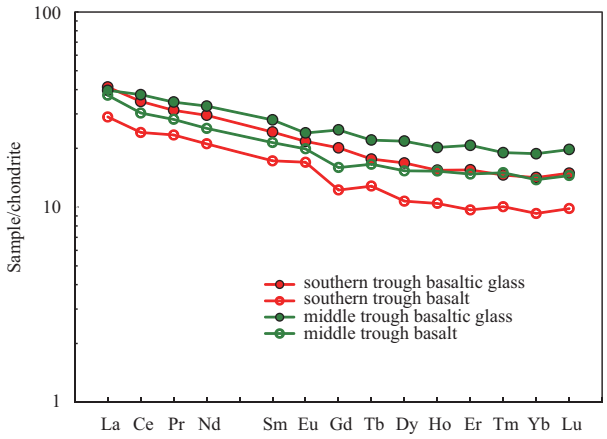

Fig. 5. Chondrite-normalized diagram of trace elements in basalt and basaltic glass samples from the OT (Sun and McDonough, 1989)

mantle source (Guo et al., 2016). Other important reasons might be the mantle heterogeneity and different degrees of magmatic evolution (Ma et al., 2004).

5.2 *Magmatic evolution*

The basalts in the OT are the products of primary magma that has undergone a certain degree of crystallization differentiation (Zhai and Gan, 1995). Different MgO contents in the basalts of the middle and SOT indicate that they undergone crystallization differentiation in different degrees. While plagioclase crystallizes and separates, a negative Eu anomaly is generated (Henderson, 1984). The results of this study show that Eu proportions in the basalts of the OT manifest as a tiny positive anomaly, while the basaltic glass contains few, or no, such anomaly (Fig. 5). It indicates that crystallization of plagioclase occurs in basaltic magma though this process may not be distinct from the magmatic system. The trace element Sr has similar characteristics to Eu as it easily enters into the plagioclase resulting in another anomaly. Our results show that a positive Sr anomaly is present in the basalts from MOT, while no such discrepancy is present in basaltic glass (Fig. 4). It indicates that crystallization of plagioclase occurs in the magmas from MOT and there is no or part of plagioclase to separate from the magmatic system. Most plagioclase remains within the magmatic system. In addition, the negative Ti anomaly in the trace element spider diagram for basalts and basaltic glass are the result of crystal separation of spinels and magnetite (or titanomagnetite).

The MgO content of basaltic magmas can be used to indicate liquidus or eruption temperature, as well as to understand variations in magma composition during the cooling process alongside variations in the oxides of major elements (i.e., Al_2O_3, FeO, CaO, Na_2O, TiO_2, and MnO) (Niu et al., 2002; Niu, 2013). Thus, in MgO-Al_2O_3 diagram (Fig. 7a), the results show that the Al_2O_3 content of basaltic glass is lower than that of OT whole rock samples,

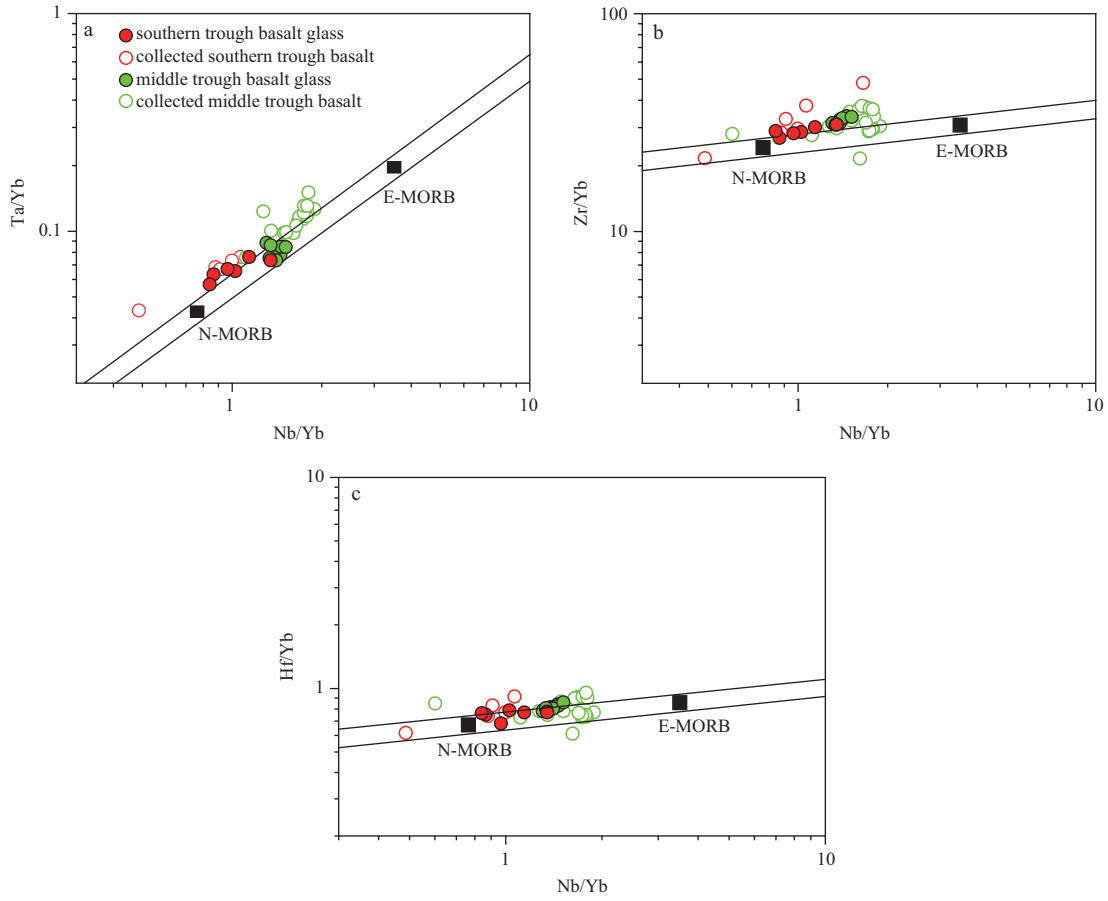

Fig. 6. Diagrams of Ta/Yb-Nb/Yb (a), Zr/Yb-Nb/Yb (b), and Hf/Yb-Nb/Yb (c) in OT basaltic glass samples. Data of N-MORB and E-MORB is from Sun and McDonough (1989). Data of the Okinawa Trough basalt is from Li et al. (1997a, b), Shinjo et al. (1999), Ma et al. (2004), and Hoang and Uto (2006).

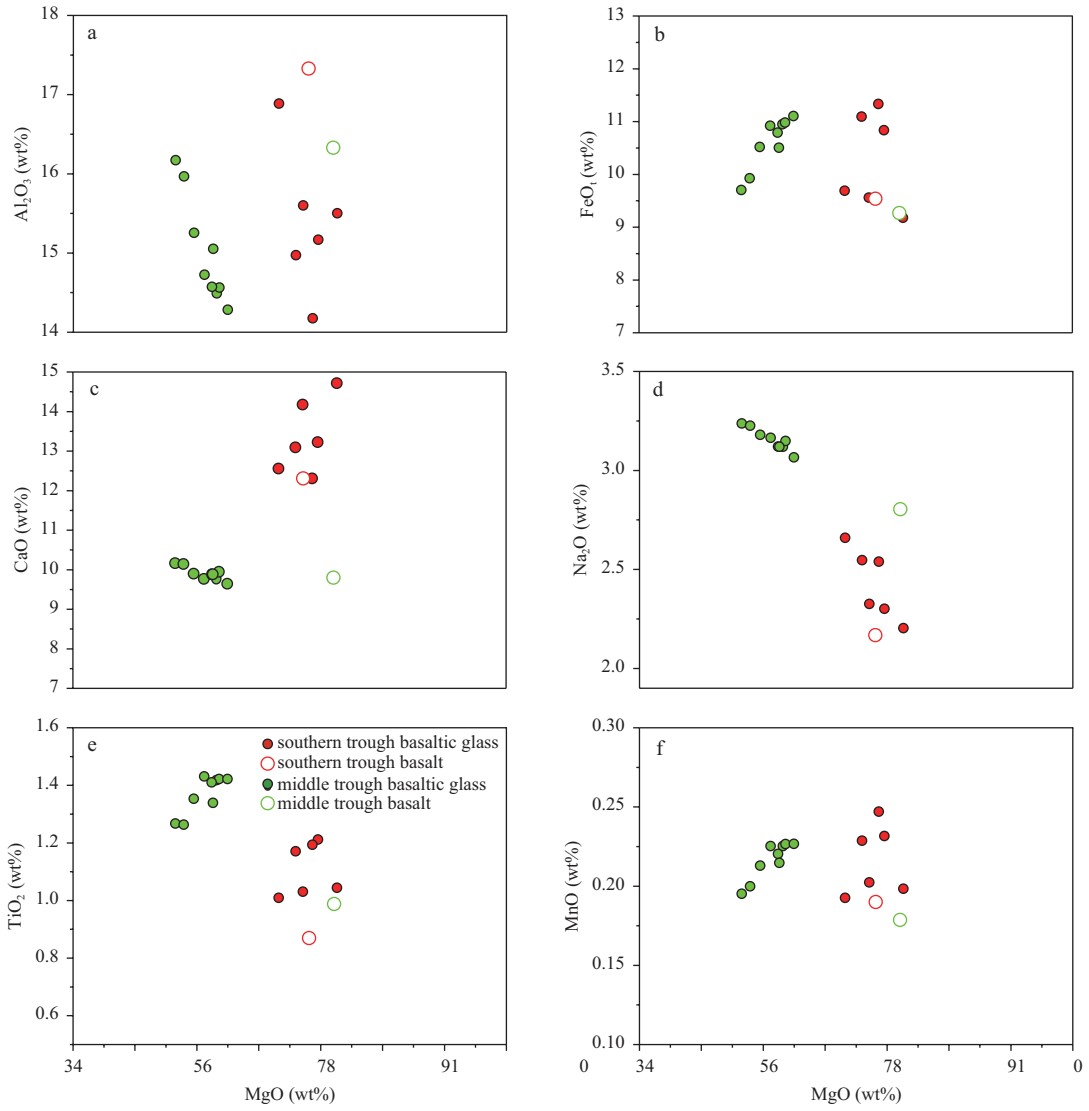

Fig. 7. Relationships between MgO and various oxides in OT basaltic glass and basalt samples.

indicative of plagioclase crystallization. As MgO decreases, the proportion of Al_2O_3 in basaltic glass from MOT increases, which indicates that the main crystalline mineral in the magmatic system is not plagioclase. The relative contents of basaltic minerals (i.e., plagioclases comprise 10% of phenocrysts, while pyroxenes account for 40%; Zhai and Gan, 1995) also show that crystallization of plagioclase is less than that of pyroxene. Because the existence of H_2O can restrict crystallization of plagioclase (Taylor and Martinez, 2003), the clinopyroxene crystallizes at an earlier stage (Sisson and Grove, 1993). The MgO-Al_2O_3 diagram in this study shows that crystallization of plagioclase in the magma source of MOT is restricted. At the same time, the MgO-FeOt diagram (Fig. 7b) shows that the proportion of the latter is higher in OT basaltic glass than whole rock samples which indicates a cessation of olivine and spinel crystallization. As these minerals are both rich in FeOt, crystallization must result in the reduction of this molecule in the basaltic glass component of the magmatic system. In the MgO-TiO_2 diagram (Fig. 7e), content of the latter in the basaltic glass component is higher than that in whole rock samples, which also indicates a cessation of spinel crystallization (i.e., average TiO_2 content in spinel is 1.9%; Zhai and Gan, 1995).

The proportions of FeOt and TiO_2 in basaltic glass from MOT are positively correlated with MgO contents (Figs 7b and e), which indicates that the magmatic system falls within the pyroxene and magnetite (or titanomagnetite) crystallization period. Variations of CaO and MgO in basaltic glass from MOT are indicative of clinopyroxene crystallization (Fig. 7c); indeed, as crystallization of plagioclase is restricted, CaO should exhibit a similar negative correlation with Al_2O_3. However, the variations reported here suggest that as crystallization of clinopyroxene decreases the CaO content in glass should increase. As the CaO content in basaltic glass from SOT is higher than that of whole rock samples, this result demonstrates that crystallization is dominated by neither plagioclase or pyroxene, but olivine (SiO_2 content in basalts from SOT is 48.94%, indicative of a relatively earlier period of magmatic evolution; Li et al., 1997b). This is likely because either plagioclase or clinopyroxene crystallization can lead to a decrease in the CaO content of basaltic glass.

In conclusion, it is clear that the basalts in MOT have experienced more crystallization than their counterparts in SOT and that the entire magmatic system is oriented towards pyroxenes. Crystallization of plagioclase was restricted by H_2O to some extent, while crystallization of spinel and olivine stopped entirely. The evolution of basalt crystallization in SOT has been domin-

ated by olivine.

5.3 *Subducted components*

One of the most important characteristics of BABBs is the existence of a subducted component. Although the effect of this component is smaller than the case in IABs, it is nevertheless obvious (Pearce and Stern, 2006); the spider diagram of basalt trace elements for samples from the OT (Fig. 4) demonstrates similar enrichment characteristics for Rb, Ba, Th, U, and K with basalts from other back-arc basins (e.g., the Mariana Trough and Lau Basin). Differences in spider diagram patterns between basalts from southern and MOT also illustrate variation in the effects of subduction of the Philippine Sea Plate on segments of the OT. For example, Pearce et al. (2005) interpreted the pattern of trace elements in the IABs of the Mariana Trench as comprising a mantle component defined by immobile subduction, a subducted fluid component defined by Rb, Ba, K, Sr, and Pb, and a subducted melt component defined by Th, U, and LREEs, and Ba, Th, and Nb exhibit similar partitioning coefficients in partial melting and crystallization differentiation processes (Pearce and Stern, 2006), while normalization using Yb enables discussion of the contribution of subducted components to basalts of the OT as well as effects on magmatic processes.

Pearce and Stern (2006) also suggested that while Th is immobile in low-temperature aqueous fluids, and mobile in high-temperature melts. So, the addition of Th (pink arrow in Fig. 8a) indicates influence of subducted melts. The results presented in Fig. 8a shows 50%–70% Th in the magma source of the MOT, while about 90% of this element in the southern magma source are derived from subducted components. Both SOT and MOT basalts are shown more subducted melt component influence (higher subduction-derived Th and Ba) than LBB and MTB. Indeed, the element Ba is mobile in both subducted fluids and melts. Hence, the addition of Ba (pink arrows direction in Fig. 8b) indicates total subducted component influence to a back-arc basin. The results presented in Fig. 8b show that 70%–90% Ba in the magma source of the MOT and 95% in the southern source region are derived from a subducted component. The addition of total subducted component in OT is similar to LBB and MTB.

The magma source of the southern OT has been influenced more by subducted components, while Ba/Th and Th/Nb were selected as proxies for the effects of subducted fluids and melts, respectively. The data presented in Fig. 9 shows that the effect of a subducted fluid component to the magma source of the OT is obviously smaller than that of other back-arc basins, while the effects of subducted fluid components to SOT and MOT are almost the same. The effect of subducted melt components to the magma source of the MOT is similar to that in other back-arc basins, while the effect in SOT is clearly larger than other basins as well as the MOT. Different subducted component influence in these troughs and basins may be due to different subduction zone structural feature (Zheng et al., 2016), such as geothermal gradient, subduction rate and angle.

6 Conclusions

(1) Basalts in MOT and SOT both exhibit features characteristic to iron-rich tholeiite series. Trace elements in these samples conform to the typical spider diagram pattern seen in BABBs and are rich in LILEs, including Rb, Ba, Pb, U, and Th, while at the same time are depleted in HFSEs, including Nb, Ta, Zr, Hf, and Ti. REEs in these samples exhibit typical right-leaning LREE enrichment characteristics.

(2) The magma source of the OT is N-MORB-type mantle, richer in the middle of this region than in the south. The addition of EMI-type mantle material as well as heterogeneity may have led to variable degrees of enrichment in different regions of the OT.

(3) The magma source for the MOT is characterized by a crystallization evolution oriented towards pyroxenes. This means that crystallization of plagioclase was restricted, while spinel and olivine crystallization ceased entirely. At the same time, while crystallization of the southern magma source was dominated by

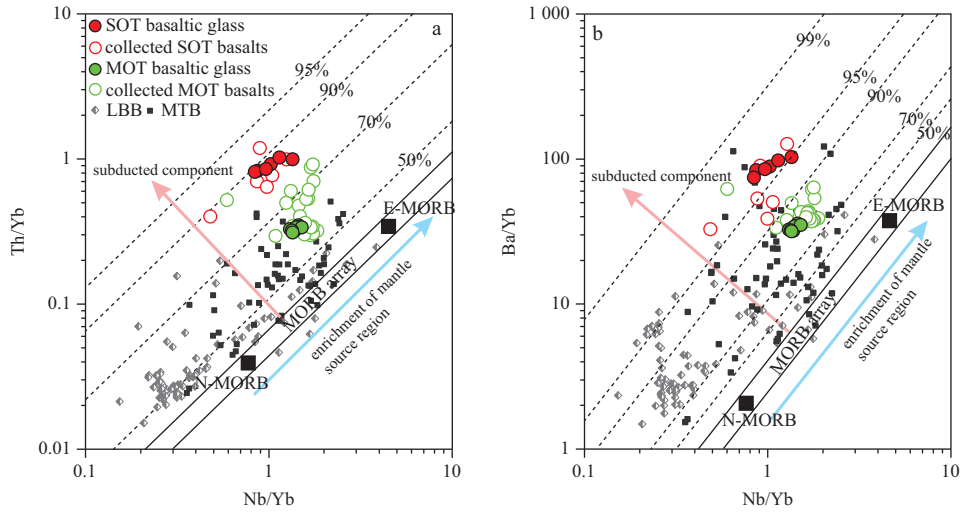

Fig. 8. Diagrams to show Nb/Yb-Th/Yb (a) and Nb/Yb-Ba/Yb (b) in OT basalts and basaltic glass samples. Dashed line parallel to the MORB arrays on plot refers to the percentage of subduction-derived element Th in the mantle source, assuming that Nb is subduction-immobile element. LBB means Lau basin basalts and MTB Mariana Trough basalts. The pink arrow represents subduction component addition and blue arrow enrichment of mantle source. Data of N-MORB and E-MORB is from Sun and McDonough (1989). Data of Okinawa Trough basalt is from Li et al. (1997a, b), Shinjo et al. (1999), Ma et al. (2004), and Hoang and Uto (2006). Data of Lau Basin basalts is from Peate et al. (2001), Fretzdorff et al. (2006), Tian et al. (2008), and Yan et al. (2012). Data of Mariana Trough basalts is from Hawkins et al. (1990) and Pearce et al. (2005).

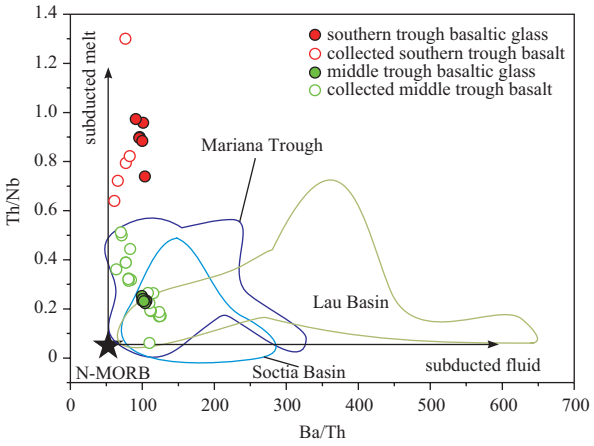

Fig. 9. Diagram to show Ba/Th-Th/Nb in OT basalt and basaltic glass samples. Data of OT basalt and N-MORB is same as Fig. 8. Data of Lau Basin basalts is from Peate et al. (2001), Fretzdorff et al. (2006), Tian et al. (2008), and Yan et al. (2012). Data of Mariana Trough basalts is from Hawkins et al. (1990) and Pearce et al. (2005). Data of Soctia Basin basalts is from Leat et al. (2000).

olivine, this also included components of plagioclase, pyroxene, and magnetite (i.e., titanomagnetite).

(4) The results of this study show that 90% Th and 95% Ba in basalts in SOT originated from subducted components, while 50%–70% Th and 70%–90% Ba in basalts in MOT are derived from these components. The distribution of subducted components across the OT also varies; data show that SOT was influenced more by components of subducted melt, while the influence of subducted fluids in SOT and MOT were almost the same. These effects, however, were obviously smaller than those seen in basalts from other back-arc basins.

Acknowledgements

The authors thank Liu Guoqi for help with sample analysis. All authors are thankful to two anonymous reviewers for the thorough revision of the manuscript and their insightful comments.

References

Chen Xiaoming, Tan Qingquan, Zhao Guangtao. 2002. Plagioclases from the basalt of Okinawa Trough and its petrogenesis significance. Acta Petrologica Sinica (in Chinese), 18(4): 482–488

Eissen J P, Lefèvre C, Maillet P, et al. 1991. Petrology and geochemistry of the central North Fiji Basin spreading centre (Southwest Pacific) between 16°S and 22°S. Marine Geology, 98(2-4): 201–239

Fretzdorff S, Livermore R A, Devey C W, et al. 2002. Petrogenesis of the back-arc East Scotia Ridge, South Atlantic Ocean. Journal of Petrology, 43(8): 1435–1467

Fretzdorff S, Schwarz-Schampera U, Gibson H L, et al. 2006. Hydrothermal activity and magma genesis along a propagating back-arc basin: Valu Fa Ridge (southern Lau Basin). Journal of Geophysical Research, 111(B8): B08205

Gaetani G A, Grove T L, Bryan W B. 1993. The influence of water on the petrogenesis of subductionrelated igneous rocks. Nature, 365(6444): 332–334

Gaetani G A, Grove T L. 1998. The influence of water on melting of mantle peridotite. Contributions to Mineralogy and Petrology, 131(4): 323–346

Guo Kun, Zhai Shikui, Yu Zenghui, et al. 2016. Sr-Nd-Pb isotopic geochemistry of phenocrysts in pumice from the central Okinawa Trough. Geological Journal, 51(S1): 368–375

Hawkins J W, Lonsdale P F, Macdougall J D, et al. 1990. Petrology of the axial ridge of the Mariana Trough backarc spreading center. Earth and Planetary Science Letters, 100(1-3): 226–250

Hawkins J W, Melchior J T. 1985. Petrology of Mariana trough and Lau basin basalts. Journal of Geophysical Research, 90(B13): 11431–11468

Henderson P. 1984. Rare Earth Element Geochemistry. Amsterdam: Elsevier Press

Hoang N, Uto K. 2006. Upper mantle isotopic components beneath the Ryukyu arc system: evidence for 'back-arc' entrapment of Pacific MORB mantle. Earth and Planetary Science Letters, 249(3-4): 229–240

Honma H, Kusakabe M, Kagami H, et al. 1991. Major and trace element chemistry and D/H, $^{18}O/^{16}O$, $^{87}Sr/^{86}Sr$ and $^{143}Nd/^{144}Nd$ ratios of rocks from the spreading center of the Okinawa Trough, a marginal back-arc basin. Geochemical Journal, 25(2): 121–136

Huang Peng, Li Anchun, Jiang Hengyi. 2006. Geochemical features and their geological implications of volcanic rocks from the northern and middle Okinawa Trough. Acta Petrologica Sinica (in Chinese), 22(6): 1703–1712

Ishizuka H, Kawanobe Y, Sakai H. 1990. Petrology and geochemistry of volcanic rocks dredged from the Okinawa Trough, an active back-arc basin. Geochemical Journal, 24(2): 75–92

Ishizuka O, Yuasa M, Taylor R N, et al. 2009. Two contrasting magmatic types coexist after the cessation of back-arc spreading. Chemical Geology, 266(3-4): 274–296

Karig D E. 1971. Origin and development of marginal basins in the western Pacific. Journal of Geophysical Research, 76(11): 2542–2561

Kimura M. 1985. Back-arc rifting in the Okinawa Trough. Marine and Petroleum Geology, 2(3): 222–240

Kimura M, Kaneoka I, Kato Y, et al. 1986. Report on DELP 1984 cruises in the middle Okinawa trough: Part V. Topography and geology of the central Grabens and their vicinity. Bulletin of the Earthquake Research Institute, University of Tokyo, 61(2): 269–3l

Leat P T, Livermore R A, Millar I L, et al. 2000. Magma supply in back-arc spreading Centre segment E2, East Scotia Ridge. Journal of Petrology, 41(6): 845–866

Li Weiran, Yang Zuosheng, Wang Yongji, et al. 1997a. The petrochemical features of the volcanic rocks in Okinawa Trough and their geological significance. Acta Petrologica Sinica (in Chinese), 13(4): 538–550

Li Weiran, Yang Zuosheng, Zhang Baomin, et al. 1997b. Study on the olivine tholeiite of the southern Okinawa Trough. Oceanologia et Limnologia Sinica (in Chinese), 28(6): 665–672

Liu Yongsheng, Gao Shan, Hu Zhaochu, et al. 2010a. Continental and oceanic crust recycling-induced melt-peridotite interactions in the Trans-North China Orogen: U-Pb dating, Hf isotopes and trace elements in zircons from mantle xenoliths. Journal of Petrology, 51(1-2): 537–571

Liu Yongsheng, Hu Zhaochu, Zong Keqing, et al. 2010b. Reappraisement and refinement of zircon U-Pb isotope and trace element analyses by LA-ICP-MS. Chinese Science Bulletin, 55(15): 1535–1546

Liu Bo, Li Sanzhong, Suo Yanhui, et al. 2016. The geological nature and geodynamics of the Okinawa Trough, Western Pacific. Geological Journal, 51(S1): 416–428

Ma Weilin, Wang Xianlan, Jin Xianglong, et al. 2004. Areal difference of middle and southern basalts from the Okinawa Trough and its genesis study. Acta Geologica Sinica (in Chinese), 78(6): 758–769

Macdonald R, Hawkesworth C J, Heath E. 2000. The Lesser Antilles volcanic chain: a study in arc magmatism. Earth-Science Reviews, 49(1-4): 1–76

Meng Xianwei, Chen Zhihua, Du Dewen, et al. 2000. Sr, Nd isotope geochemistry of volcanic rock series and its geological significance in the middle Okinawa Trough. Science in China Series D: Earth Sciences, 43(5): 458–463

Miyashiro A. 1974. Volcanic rock series in island arcs and active continental margins. American Journal of Science, 274(4): 321–355

Niu Yaoling. 2013. Global Tectonics and Geodynamics—A Petrological and Geochemical Approach (in Chinese). Beijing: Science Press

Niu Yaoling, Regelous M, Wendt I J, et al. 2002. Geochemistry of near-EPR seamounts: importance of source vs. process and the origin of enriched mantle component. Earth and Planetary Science Letters, 199(3-4): 327–345

Pearce J A, Ernewein M, Bloomer S H, et al. 1994. Geochemistry of Lau Basin volcanic rocks: influence of ridge segmentation and arc proximity. Geological Society, London, Special Publications, 81(1): 53–75

Pearce J A, Stern R J, Bloomer S H, et al. 2005. Geochemical mapping of the Mariana arc-basin system: Implications for the nature and distribution of subduction components. Geochemistry, Geophysics, Geosystems, 6(7): Q07006

Pearce J A, Stern R J. 2006. Origin of back-arc basin magmas: trace element and isotope perspectives. In: Christie D M, Fisher C R, Lee S M, et al, eds. Back-Arc Spreading Systems: Geological, Biological, Chemical, and Physical Interactions. Washington, D C: American Geophysical Union, 63–86

Peate D W, Kokfelt T F, Hawkesworth C J, et al. 2001. U-series isotope data on Lau Basin glasses: the role of subduction-related fluids during melt generation in back-arc basins. Journal of Petrology, 42(8): 1449–1470

Rickwood P C. 1989. Boundary lines within petrologic diagrams which use oxides of major and minor elements. Lithos, 22(4): 247–263

Shinjo R, Chung S L, Kato Y, et al. 1999. Geochemical and Sr-Nd isotopic characteristics of volcanic rocks from the Okinawa Trough and Ryukyu arc: implications for the evolution of a young, intracontinental back arc basin. Journal of Geophysical Research, 104(B5): 10591–10608

Shinjo R, Kato Y. 2000. Geochemical constraints on the origin of bimodal magmatism at the Okinawa Trough, an incipient back-arc basin. Lithos, 54(3-4): 117–137

Sibuet J C, Letouzey J, Barbier F, et al. 1987. Back arc extension in the Okinawa Trough. Journal of Geophysical Research, 92(B13): 14041–14063

Sinton J M, Ford L L, Chappell B, et al. 2003. Magma genesis and mantle heterogeneity in the Manus back-arc basin, Papua New Guinea. Journal of Petrology, 44(1): 159–195

Sisson T W, Grove T L. 1993. Experimental investigations of the role of H_2O in calc-alkaline differentiation and subduction zone magmatism. Contributions to Mineralogy and Petrology, 113(2): 143–166

Sun S S, McDonough W F. 1989. Chemical and isotopic systematics of oceanic basalts: implications for mantle composition and processes. Geological Society, London, Special Publications, 42(1): 313–345

Taylor B, Martinez F. 2003. Back-arc basin basalt systematics. Earth and Planetary Science Letters, 210(3-4): 481–497

Tian Liyan, Castillo P R, Hawkins J W, et al. 2008. Major and trace element and Sr-Nd isotope signatures of lavas from the Central Lau Basin: implications for the nature and influence of subduction components in the back-arc mantle. Journal of Volcanology and Geothermal Research, 178(4): 657–670

Yan Quanshu, Castillo P R, Shi Xuefa. 2012. Geochemistry of basaltic lavas from the southern Lau Basin: input of compositionally variable subduction components. International Geology Review, 54(12): 1456–1474

Yan Quanshu, Shi Xuefa. 2014. Petrologic perspectives on tectonic evolution of a nascent basin (Okinawa Trough) behind Ryukyu Arc: a review. Acta Oceanologica Sinica, 33(4): 1–12

Yu Zenghui, Zhai Shikui, Guo Kun, et al. 2016. Helium isotopes in volcanic rocks from the Okinawa Trough—impact of volatile recycling and crustal contamination. Geological Journal, 51(S1): 376–386

Zhai Shikui, Gan Xiaoqun. 1995. Study of basalt from the hydrothermal field of the Okinawa Trough. Oceanologia et Limnologia Sinica (in Chinese), 26(2): 115–123

Zheng Yongfei, Chen Renxu, Xu Zheng, et al. 2016. The transport of water in subduction zones. Science China Earth Sciences, 59(4): 651–682